Estimation of local SAR using B1 mapping

U. Katscher[1], T. Voigt[2], C. Findeklee[1], K. Nehrke[1], S. Weiss[1], and O. Doessel[2]
[1]Philips Research Europe - Hamburg, Hamburg, Germany, [2]University Karlsruhe, Karlruhe, Germany

Introduction: The local specific energy absorption rate (SAR) is one of the major issues for MRI at 3T and above. For an exact determination of local SAR, the spatial distribution of the electric field as well as the electric conductivity distribution throughout the patient are required. Alternatively, according to Maxwell's equations, the required quantities can be deduced from the magnetic field of the RF coil. In this study, the local SAR is estimated via suitable post-processing of a standard B1 map. Simulations show, that the information content of a B1 map might be sufficient to estimate a local SAR close to the correct local SAR.

Theory: Faraday's law in integral form is given by

$$-i\omega\mu\int_A \underline{\vec{H}}\,\mathrm{d}\vec{a} = \oint_{\partial A} \underline{\vec{E}}(\vec{r})\cdot\mathrm{d}\vec{r} \qquad (1)$$

with $\underline{\vec{H}}$ the magnetic field strength, $\underline{\vec{E}}$ the electric field, ω the Larmor frequency, A the integration area and ∂A the curve along the integration area. The underlinings denote complex variables. On the other hand, Ampere's law in differential form can be written as

$$\nabla\times\underline{\vec{H}}(\vec{r})/i\omega = \underline{\varepsilon}(\vec{r})\underline{\vec{E}}(\vec{r}) \qquad (2)$$

Here, $\underline{\varepsilon} = \varepsilon - i\sigma/\omega$ denotes the (supposed to be isotropic) complex permittivity, ε the scalar permittivity, and σ the electric conductivity. To estimate $\underline{\varepsilon}$, Eq. (2) is integrated along ∂A and divided by Eq. (1)

$$\oint_{\partial A}\nabla\times\underline{\vec{H}}(\vec{r})\cdot\mathrm{d}\vec{r}\Big/\mu\omega^2\int_A\underline{\vec{H}}\,\mathrm{d}\vec{a} = \oint_{\partial A}\underline{\varepsilon}(\vec{r})\underline{\vec{E}}(\vec{r})\cdot\mathrm{d}\vec{r}\Big/\int_{\partial A}\underline{\vec{E}}(\vec{r})\cdot\mathrm{d}\vec{r} \approx \underline{\varepsilon}(\vec{r}) \qquad (3)$$

This estimation is valid in regions, where the spatial variation of $\underline{\varepsilon}$ along ∂A is significantly smaller than the variation of $\underline{\vec{E}}$, e.g., inside compartments with constant $\underline{\varepsilon}$.

From this result, local SAR can be estimated via an integral over the corresponding local region V

$$SAR_{local} = \int_V \sigma(\vec{r})\underline{\vec{E}}(\vec{r})\underline{\vec{E}}^{*}(\vec{r})\mathrm{d}v \cdot \qquad (4)$$

For this equation, σ is taken from Eq. (3) and $\underline{\vec{E}}$ from dividing Eq. (2) by Eq. (3). For Eq. (3), all three spatial components of the magnetic field are required. In principle, $\underline{H}_x$ and $\underline{H}_y$ can be measured via MRI by utilizing the sensitivities $\underline{H}^+$ and $\underline{H}^-$ of an RF coil for the transmit and receive case, respectively

$$\underline{H}^+ = \left(\underline{H}_x + i\underline{H}_y\right)/2 \;\;,\;\; \underline{H}^- = \left(\underline{H}_x - i\underline{H}_y\right)/2 \cdot \qquad (5)$$

For this study, a birdcage is used, for which $\underline{H}^- = 0$ can be assumed [1] due to $\underline{H}^+ >> \underline{H}^-$. However, no method has been published to determine the component $\underline{H}_z$ parallel to the main field. Three possible estimations are: (*i*) Derive $\underline{H}_z$ from a full model of the used RF coil and the patient. This yields local SAR, which suffers only from model errors and numerical errors (e.g., from imperfect numerical differentiation). However, the setup of the full model is highly sophisticated. This approach would be equivalent to "Electric Properties Tomography" [1]. (*ii*) Derive $\underline{H}_z$ from an RF coil model only. Thus, besides model and numerical errors, also a systematic error is introduced. However, the setup of a coil model only is much easier than modeling also the patient. (*iii*) Use of a constant $\underline{H}_z$ or $\underline{H}_z = 0$. This, of course, further increases the systematic error. However, no model at all is needed, which would enhance the practicability of the method significantly. It is expected, that transverse slices (corresponding to a transverse orientation of A and ∂A) suffer most from simplifications of $\underline{H}_z$ due to the division by the integrated $\underline{H}_z$ in this slice orientation. To avoid this problem, only coronal slices are investigated in this study.

Methods: Electro-magnetic fields of coronal slices have been simulated using a finite-difference time-domain (FDTD) method ("XFDTD", Remcom, Inc., USA) for a quadrature body coil (QBC) at 3T and a bio-mesh model of the "Visible Human Male" (National Library of Medicine, Bethesda, USA) with a resolution of 5mm (Fig. 1). The fields have been used as input for the three described cases (*i*)-(*iii*). Numerical differentiation has been performed using Savitzky-Golay coefficients considering only adjacent pixels [2]. The numerical integration area has been 3×3 pixels.

Results / Discussion: Local SAR distributions resulting from the three different approximations of $\underline{H}_z$ (*i*)-(*iii*) are shown in Fig. 2. The local SAR distribution for case (*i*) using the correct $\underline{H}_z$ is predominantly influenced by errors from the numerical differentiation and integration, particularly along the compartment boundaries. These errors can be lowered by more sophisticated numerical differentiation / integration algorithms based and a higher spatial resolution. The assumption made in Eq. (3) also contributes to the error along compartment boundaries, but is valid inside the compartments due to constant $\underline{\varepsilon}$. Small differences between the cases (*i*) and (*ii*), most prominent in regions close to the QBC, demonstrate the influence of the patient on $\underline{H}_z$. Even smaller differences are found between (*ii*) and (*iii*). The approach benefits from the fact, that in the QBC $\underline{E}_z >> \underline{E}_x$ and $\underline{E}_z >> \underline{E}_y$, and thus, local SAR is dominated by $\underline{E}_z$. However, the *z*-component of Eq.(2), from which $\underline{E}_z$ is taken, is not influenced by $\underline{H}_z$, and thus, not influenced by simplifications of $\underline{H}_z$. Fig. 3 shows profiles corresponding to Fig. 2.

Conclusion: A method is presented estimating the local SAR from B1 maps, which can be measured using standard techniques on a clinical MR scanner (see, e.g., [3,4]). Corresponding simulations show, that the presented method can estimate local SAR with a high accuracy. The method needs to be evaluated *in vivo*.

Fig. 1: Electric conductivity distribution of patient model.

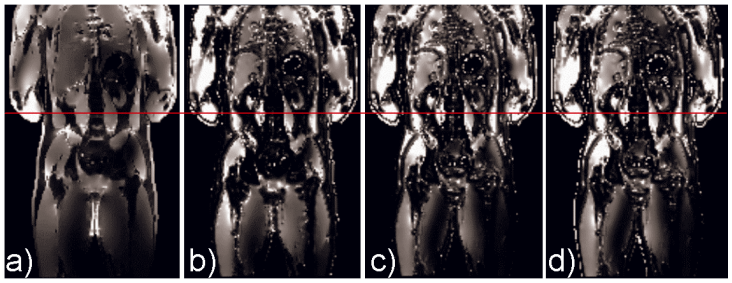

Fig. 2: Local SAR of patient model shown in Fig. 1. (a) Results from FDTD, (b) case (i) using the correct $\underline{H}_z$, (c) case (ii) using $\underline{H}_z$ of an empty coil (correlation with (i) = 98.2%), (d) case (iii) using $\underline{H}_z$ = 0 (correlation with (i) = 98.1%).

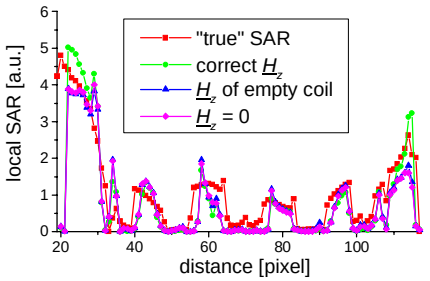

Fig. 3: Local SAR profiles along red line indicated in Fig. 2. The three discussed cases of $\underline{H}_z$ are compared to the "true" local SAR distribution determined via FDTD.

Acknowledgment The authors would like to cordially thank Dennis Gläsel for providing the electro-magnetic field data.

References [1] Katscher U et al., Proc. ISMRM 14 (2006) 3035,3037 [2] Press WH et al., *Numerical Recipes in C*. Cambridge University Press, 1995 [3] Stollberger R et al., MRM 35 (1995) 246 [4] Yarnykh VL, MRM 57 (2007) 192-200